Accounting for 16S rRNA copy number prediction uncertainty and its implications in bacterial diversity analyses

Yingnan Gao[1], yg5ap@virginia.edu

Martin Wu[1]*, mw4yv@virginia.edu

[1]Department of Biology, University of Virginia, 485 McCormick Road, Charlottesville, VA, 22904, USA

*Corresponding author

Abstract

Background: 16S rRNA gene has been widely used in bacterial and archaeal diversity studies to determine the community composition and structure. 16S rRNA gene copy number (16S GCN) varies among bacterial species and this variation introduces biases to the relative cell abundance estimated using 16S rRNA read counts. To correct the biases, methods have been developed to predict 16S GCN. 16S GCN predictions come with inherent uncertainty, which is often ignored in the downstream analyses. However, a recent study suggests that the uncertainty can be so great that copy number correction is not justified in practice. Despite the significant implications in 16S rRNA based bacterial diversity studies, the uncertainty associated with 16S GCN predictions has not been well characterized and its impact on bacterial diversity studies needs to be investigated.

Results: Here we develop RasperGade16S, a novel method and software to better model and capture the inherent uncertainty in 16S rRNA GCN prediction. RasperGade16S implements a maximum likelihood framework of pulsed evolution model and explicitly accounts for intraspecific GCN variation and heterogeneous GCN evolution rates among species. Using cross validation, we show that our method provides robust confidence estimates for the GCN predictions and outperforms other methods in both precision and recall. We have predicted GCN for 592605 OTUs in the SILVA database and tested 113842 bacterial communities that represent an exhaustive and diverse list of engineered and natural environments. We found that the prediction uncertainty is small enough for 99% of the communities that 16S GCN correction should improve their compositional and functional profiles estimated using 16S rRNA reads. On the other hand, we found that GCN variation has limited impacts on beta-diversity analyses such as PCoA, PERMANOVA and random forest test.

Conclusion: We have developed a method to accurately account for uncertainty in 16S rRNA GCN predictions and the downstream analyses. For almost all 16S rRNA surveyed bacterial communities, correction of 16S GCN should improve the results when estimating their compositional and functional profiles. However, such correction is not necessary for beta-diversity analyses.

Keywords: 16S rRNA gene copy number, confidence estimates, *RasperGade16S*, hidden state prediction, bacterial composition

Background

The 16S ribosomal RNA (16S rRNA) gene is the gold standard for bacterial and archaeal diversity study and has been commonly used to estimate the composition of bacterial and archaeal communities through amplicon sequencing. Sequence reads are usually matched to reference databases like SILVA [1] and GreenGenes [2] to determine the presence of taxa and their relative cell abundances. However, the 16S rRNA gene copy number (GCN) can vary from 1 to more than 15 [3,4] and this large copy number variation introduces bias in the relative cell abundance estimated using the gene read counts (thereafter referred to as gene abundance) [5], and consequently it can skew the community profiles, diversity measures and lead to qualitatively incorrect interpretations [5–8]. As a result, it has been argued that 16S rRNA GCN variations should be taken into account in 16S rRNA gene-based analyses [5].

The majority of bacteria species have not been cultured or sequenced and their 16S rRNA GCNs are unknown. Studies have shown that 16S rRNA GCN exhibits a strong phylogenetic signal

[5,7], and therefore 16S rRNA GCN can be inferred from closely related reference bacteria. Based on this principle, software has been developed to predict the 16S rRNA GCN [5,7,9,10] in a process often referred to as hidden state prediction [11]. However, a recent study correctly points out that the accuracy of 16S rRNA GCN prediction deteriorates as the minimum phylogenetic distance between the query sequence and the reference sequences increases, and the prediction of 16S rRNA GCN is still an open question [12].

The increasing error of 16S rRNA GCN prediction with increasing phylogenetic distance roots from the stochastic nature of trait evolution, which leads to inherent uncertainty in the predicted trait values. One way of reducing the inherent uncertainty is to improve taxon sampling in the reference phylogeny to reduce the query's phylogenetic distance to the reference [13]. Another way of addressing the inherent uncertainty is to model the uncertainty directly and have a confidence estimate. By doing so, we will be able to determine how confident we should be about a GCN prediction and make meaningful interpretations. Unfortunately, few 16S rRNA GCN prediction tools provide a confidence estimation for the predicted 16S rRNA GCN, and uncertainty is mostly ignored when interpreting the results of downstream analyses [5,7,10]. For example, PICRUST2 predicts functional profiles of bacterial and archaeal communities from 16S rRNA sequence data. It predicts 16S rRNA GCN for each operational taxonomic unit (OTU) in the community and uses the predicted values (point estimates) to estimate "corrected" relative cell abundances and metagenomes, without accounting for the uncertainty of the predictions. As a result, the impact of uncertainty in 16S rRNA GCN prediction on bacterial diversity analyses remains unknown and needs to be investigated.

Several points need to be considered to properly model the prediction uncertainty. First, because the uncertainty roots from the stochastic nature of trait evolution, we need to develop a good model for 16S rRNA GCN evolution. Previously the evolution of the 16S rRNA GCN trait has been modeled as gradual evolution using the Brownian motion (BM) model [5,7,10]. However, alternative models exist and need to be considered [14–16]. For example, the Ornstein-Uhlenbeck model assumes a centralizing trend towards an optimum [14,15]. As 16S rRNA GCN has been linked to the ecological strategy of bacterial species [17,18] and bacteria diversify across all types of environments, a consistent trend in the evolution of 16S rRNA GCN is unlikely. Thus, a model without any trend like the BM model is preferred. Pulsed evolution (PE) is another model that assumes no trend in evolution. Unlike the BM model, where small trait changes accumulate over time, the PE model postulates that traits evolve by jumps, followed by periods of stasis [14,19]. Previous studies have showed that pulsed evolution is prevalent in the evolution of mammalian body size [14,20]. It has been shown that 16S rRNA GCN of *Bacillus subtilis* can jump from 1 to 6 in a matter of days by gene amplification [21]. On the other hand, it is well known that the 16S rRNA GCN of some bacterial clades such as the Rickettsiales order, a diverse group of obligate intracellular bacteria, has only one copy of 16S rRNA in their genomes, demonstrating stasis [22,23]. To develop a proper model for 16S rRNA GCN evolution, the tempo and mode of evolution need to be examined.

Secondly, 16S rRNA GCN can vary within the same species [24–27], which introduces uncertainty to GCN prediction that needs to be accounted for. It has been shown that modeling the intraspecific variation is essential for the analysis of comparative trait data and failing to account for this variation can result in model misspecification [14]. Because conspecific strains

are usually separated by zero branch length in the phylogeny of the 16S rRNA gene, the intraspecific variation can be modelled as time-independent variation, which can also account for measurement errors [20].

Thirdly, there is notable rate heterogeneity in 16S rRNA GCN evolution. For example, the obligately intracellular bacteria and free-living bacteria with streamlined genomes (e.g., *Rickettsia* and *Pelagibacter*) have elevated molecular evolutionary rates [28,29] and therefore relatively long branches in the 16S rRNA gene phylogeny [30]. Nevertheless, they have only one copy of 16S rRNA in their genomes and the GCNs rarely change [23]. It is expected that the 16S rRNA GCN prediction for this group of bacteria should be accurate despite their large phylogenetic distances to the reference genomes. Such examples suggest that the rate heterogeneity of 16S rRNA GCN evolution should be systematically evaluated and modelled properly. However, no previous methods have evaluated and modeled such rate heterogeneity, leading to potential model misspecification in 16S rRNA GCN predictions.

Here, we develop a novel tool *RasperGade16S* that employs a heterogeneous pulsed evolution model for 16S rRNA GCN prediction. Using simulation and cross-validation, we show that *RasperGade16S* outperforms other methods in terms of providing significantly improved confidence estimates. We show that even if we cannot eliminate the inherent uncertainty of 16S rRNA GCN prediction, having an accurate confidence estimate allows us to incorporate it in downstream analyses and therefore to make better inferences from the results with confidence intervals. We show that correcting 16S rRNA GCN improves the relative cell abundance estimates of the bacterial communities and is beneficial for the vast majority of environmental

samples we have analyzed. We also show that GCN correction is unnecessary for beta-diversity analyses because it has limited impact on the results.

Methods

Preparing reference genomes and the 16S rRNA reference phylogeny

We downloaded annotated RNA gene sequences from 21245 complete bacterial genomes in the NCBI RefSeq database (Release 205) on April 9, 2021. For each genome, we counted the number of genes whose products are annotated as 16S rRNA genes. For genomes with multiple copies of 16S rRNA gene, we aligned the 16S rRNA sequences using MAFFT [31] (with parameters: --maxiterate 1000 --globalpair) and picked the 16S rRNA gene sequence that has the highest average similarity (calculated as the proportion of identical bases in the alignment) to other 16S rRNA gene sequences in the genome as the representative sequence. To remove potential errors introduced by mis-assembled genomes [32], we removed genomes whose 16S rRNA GCN differs from their 5S rRNA GCN (counted using the same strategy as 16S rRNA GCN) by greater than 2 copies, genomes whose 16S rRNA sequence contains ambiguous bases, or genomes on the list of withheld genomes in the curated ribosomal RNA operon copy number database rrnDB [3]. The 17 genomes in the rrnDB withheld list are rejected from rrnDB because their 16S rRNA genes are missing, the 16S rRNA GCNs are too high, or the genomes have inconsistent meta data (https://rrndb.umms.med.umich.edu/withheld/). We aligned the remaining representative 16S rRNA gene sequences using HMMER version 3.2 [33] (hmmalign with parameters: --trim --dna –mapali) with the hidden Markov model (HMM) built from the GreenGenes 13.8 16S rRNA gene alignment (hmmbuild with default parameters), and trimmed the alignment with a mask from the GreenGenes database [2]. The HMM, profile alignment and

the alignment mask are included in the R package RasperGade16S. After collapsing identical 16S rRNA alignments, 6408 representative sequences remained. They serve as the reference sequences and their taxonomies of are summarized in Table S1. We built a reference tree from the trimmed alignment using RAxML version 8.2 [34] with options -f d -m GTRGAMMA. We used the Deinococcus-Thermus group to root this reference phylogeny. To examine the effect of sequence alignment on model fitting, we also used the 16S rRNA HMM profile from the software Barrnap [35] to align the 16S rRNA genes (hmmalign with default parameters). We trimmed the alignment using a consensus posterior probability threshold of 0.95 (esl-alimask with parameters: -p --ppcons 0.95) and made a 16S rRNA phylogeny as described above.

Evaluating time-independent variation in 16S rRNA GCN

To evaluate the extent of 16S rRNA GCN intraspecific variation, we compared GCN between 5437 pairs of genomes with identical 16S rRNA gene alignments. To formally test whether accounting for time-independent variation is necessary, we modeled time-independent variation as a normal white noise, and fitted the Brownian motion (BM) model to the evolution of 16S rRNA GCN in the 6408 reference genomes, with and without time-independent variation. We then calculated the likelihood and chose the best model using the Akaike Information Criterion (AIC).

Evaluating the rate heterogeneity of 16S rRNA GCN evolution

To estimate the degree of rate heterogeneity in 16S rRNA GCN evolution, we calculated the local average rate of evolution for each genus that contains at least 10 genomes in the reference phylogeny and examined the distribution of the average rates among genera. The average rate of

a genus is calculated as the variance of phylogenetically independent contrasts (PICs) [36] of GCN within the genus.

Modeling 16S rRNA GCN evolution with homogeneous and heterogeneous pulsed evolution models

Using the R package *RasperGade* [37], we fitted one PE model to the entire reference phylogeny and calculated the likelihood of this homogeneous PE model. An analysis of the variance of the PICs associated with each genus indicated that there is a slowly-evolving group and a regularly-evolving group, with the average rate of the slowly-evolving group estimated to be at least 100-fold lower than that of the regularly-evolving group (Figure S1). To model the rate heterogeneity, we created two PE models: $PE_{regular}$ for the regularly-evolving group and PE_{slow} for the slowly-evolving group. We then use a two-step iterative binning procedure to estimate the parameters of $PE_{regular}$ and PE_{slow} (i.e., jump size and frequency). The $PE_{regular}$ model was initiated to take the parameter values of the homogeneous PE model. PE_{slow} was initiated to have a jump size equal to that of $PE_{regular}$ but a jump frequency100-fold lower. In our first round of binning, from the root to the tip of the reference phylogeny, we classified each node into the regularly- or slowly-evolving group by testing which model ($PE_{regular}$ or PE_{slow}) provided a better fit. We merged neighboring nodes belonging to the same group into one neighborhood and flipped neighborhood assignment if the flip resulted in an improved overall AIC value. After the first round of binning, we updated $PE_{regular}$ and PE_{slow} by fitting $PE_{regular}$ to nodes that were classified as regularly-evolving and PE_{slow} to slowly-evolving nodes. We used the updated models to perform a second round of binning to assign each node in the phylogeny to a group. Finally, we calculated r, the rate of evolution in each group, as the process variance per unit branch length defined in a

previous study [14]. We then rescaled the reference tree by multiplying the branches in the slowly-evolving group by the ratio $r_{slow}/r_{regular}$. To accommodate time-independent variation in the tip trait values, we calculated a branch length over which the process variance of the fitted pulsed evolution model is equal to the model's time-independent variation, and added this branch length to each tip branch. We compared the homogeneous and heterogeneous PE models by AIC.

Predicting 16S rRNA GCN

We used the R package *RasperGade16S* to predict 16S rRNA GCN using the heterogeneous pulsed evolution model. *RasperGade16S* first assigns the query sequence to either the regularly-evolving or the slowly-evolving group based on where it is inserted in the reference phylogeny. For a query sequence inserted into the slowly-evolving group, its insertion branch length is scaled by the ratio $r_{slow}/r_{regular}$. For a query sequence inserted into the regularly-evolving group, a small branch length is added to the insertion branch to represent the estimated time-independent variation. *RasperGade16S* then predicts the GCN of the query using the rescaled reference phylogeny. Because 16S rRNA GCN is an integer trait, the continuous prediction from hidden state prediction is rounded and a confidence (probability) that the prediction is equal to the truth is estimated by integrating the predicted uncertainty distribution. We marked the 16S rRNA GCN prediction with a confidence smaller than 95% as unreliable, and otherwise as reliable. As a comparison, we also predicted GCN using PICRUST2, which employs multiple hidden state prediction methods in the R package *castor* [38] for 16S rRNA GCN predictions. We selected three methods by which confidence can be estimated: the phylogenetically independent contrast (pic) method, the maximum parsimony (mp) method, and the empirical probability (emp) method. Otherwise, we run PICRUST2 using default options and the unscaled reference

phylogeny. For the pic method, the confidence measure is not provided by the hidden state prediction function of the *castor* package, and thus we used a customized R script to reroot the tree at the query sequence and estimated the confidence of the prediction.

We did not test the tools CopyRighter [7] and PAPRICA [9] directly in this study because 1) neither provides the option of using a user-supplied reference data, and 2) neither provides uncertainty estimates (i.e., confidence intervals) of its predictions, which is the primary focus of this study. However, CopyRighter employs the pic method and we expect its performance to be highly similar to PICRUST2 running the pic method. As PAPRICA [9]employs the subtree average method, a continuous analogue to the emp method, we expect that its performance will be highly similar to that of PICRUST2 running the emp method.

Adjust NSTD and NSTI with rate heterogeneity

The adjusted nearest-sequenced-taxon-distances (NSTDs) [12] is calculated using the rescaled reference tree. The adjusted nearest-sequenced-taxon-index (NSTI) [10] is calculated as the weighted average of adjusted NSTDs of the community members.

Validating the quality of predicted 16S rRNA GCN and its confidence estimate

We used cross-validations to evaluate the quality of 16S rRNA GCN prediction and its confidence estimate, and how they vary with NSTD. We randomly selected 2% of the tips in the reference phylogeny as the test set and filtered the remaining reference set by removing tips with a NSTD to any test sequence smaller than a threshold. We then predicted the 16S rRNA GCN for each tip in the test set using the filtered reference set. We conducted cross-validation within 9

bins delineated by 10 NSTD thresholds: 0, 0.002, 0.005, 0.010, 0.022, 0.046, 0.100, 0.215, 0.464 and 1.000 substitutions/site, and for each bin we repeated the cross-validation 50 times with non-overlapping test sets. We evaluated the quality of the 16S rRNA GCN prediction by the coefficient of determination (R^2), the fraction of variance in the true copy numbers explained by the prediction. We evaluated the quality of confidence estimate by precision and recall. Precision is defined as the proportion of accurately predicted 16S rRNA GCN in predictions considered as reliable (with ≥ 95% confidence), and recall is defined as the proportion of reliable predictions in the accurately predicted 16S rRNA GCNs. We averaged the R^2, precision and recall for the 50 cross-validations in each bin.

Simulating 16S rRNA GCN variation under pulsed evolution model

To evaluate the performance of different prediction methods when the trait evolves under the pulsed evolution model, we simulated the evolution of 16S rRNA GCN using the fitted heterogeneous pulsed evolution model. Specifically, we first simulated the number of jump events for each branch in the reference phylogeny based on the rate group that branch belongs to. Then we simulated the continuous trait change for each branch using the corresponding number of jump events. We added up the continuous trait change from the root to the tips to get the tip trait values and rounded them to the nearest integers. This set of simulated 16S rRNA GCN is referred to as ST1.

Simulating bacterial communities with 16S rRNA GCN variation

To evaluate the effect of 16S rRNA GCN correction on bacterial diversity analyses, we simulated two sets of bacterial communities using the reference genomes: one set for relative cell

abundance analyses (SC1) and the other set for beta-diversity analyses (SC2). We treated each reference genome as one OTU. For SC1, we simulated a total of 100 communities. For each simulated community, we randomly selected 2000 OTUs from the reference genomes, and assigned each OTU a cell abundance randomly drawn from a log-series species abundance distribution.

In SC2, we simulated communities in two environments to evaluate the effect of 16S rRNA GCN correction on beta diversity analyses. We simulated 10 communities per environmental type and 2000 OTUs per community. We controlled the community turnover rate by controlling the number of unique OTUs in each community. For example, at a turnover rate of 10%, a community would have 200 unique OTUs and 1800 core OTUs that are shared among all communities. We varied the turnover rate from 10% to 90% at 10% intervals. To control for the effect size of environmental type, we assigned 5, 20 or 100 signature OTUs to each environmental type. These signature OTUs were shared between the two environmental types but were twice more likely to be placed in top ranks of the log-series distribution (i.e., to be more abundant) than the non-signature OTUs in their corresponding environment. The 16S rRNA GCN of each OTU was assigned randomly from the reference genomes' GCN. We simulated 50 batches of communities for each combination of turnover rate and signature OTU number, resulting in 27000 simulated communities in SC2.

Evaluating the effect of 16S rRNA GCN correction on relative cell abundance estimation

We evaluated the effect of 16S rRNA GCN correction on the simulated bacterial communities (SC1). To estimate the confidence interval (CI) of the corrected relative cell abundance of each

OTU in a community, we randomly drew 1000 sets of 16S rRNA GCNs from their predicted uncertainty distribution. For each set of 16S rRNA GCNs, we divided the gene read count of OTUs by their corresponding 16S rRNA GCNs to get the corrected cell counts. The median of the corrected cell count for each OTU in the 1000 sets is used as the point estimate of the corrected cell count, and the OTU's relative cell abundance is calculated by normalizing the corrected cell count with the sum of corrected cell counts of all OTUs in the community. The 95% CI for each OTU's relative cell abundance is determined using the 2.5% and 97.5% quantiles of the 1000 sets of corrected relative cell abundances. The OTU with the highest corrected relative cell abundance is considered the most abundant taxon. The support value for the most abundant OTU is calculated as the empirical probability that the OTU has the highest cell abundance in the 1000 sets of corrected cell abundances. We calculated the coverage probability of the CI as the empirical frequency that the relative gene abundance or true relative cell abundance is covered by the estimated CI. We evaluated the effect of 16S rRNA GCN correction on relative cell abundance estimation at different NSTD thresholds.

Evaluating the effect of 16S rRNA GCN correction on beta-diversity analyses

We used the Bray-Curtis dissimilarity, a commonly used metric in beta-diversity analyses, for any beta-diversity analysis that requires a dissimilarity matrix, and evaluated the effect of 16S rRNA GCN correction on the simulated bacterial communities (SC2). To correct for 16S rRNA GCN variation in beta-diversity analyses, we divided the gene abundance of each OTU by its predicted 16S rRNA GCN and calculated the corrected relative cell abundance table and the corresponding Bray-Curtis dissimilarity matrix. We used the corrected cell abundance table to generate the principal coordinates analysis (PCoA) plot and to conduct the permutational

multivariate analysis of variance (PERMANOVA) and the random forest test with the R package *vegan* and *randomForest*, respectively.

Predicting 16S rRNA GCN for SILVA OTUs

We downloaded 592605 full-length representative bacterial 16S rRNA sequences of non-redundant OTUs at 99% similarity (OTU99) in the SILVA release 132 [1]. We aligned and trimmed the sequences using the method described above. We then inserted the OTUs into the reference phylogeny using the evolutionary placement algorithm (EPA-ng) [39] with the model parameters estimated by RAxML when building the reference phylogeny. We limited the maximum number of placements per SILVA representative sequence to 1. We predicted the 16S rRNA GCN for each SILVA OTU99 as described above using the heterogeneous pulsed evolution model and calculated adjusted NSTDs.

Evaluating the effect of GCN correction in HMP1 and EMP dataset

To check the effect of 16S rRNA GCN correction in empirical data, we analyzed the 16S rRNA V1-V3 amplicon sequence data of the first phase of Human Microbiome Project (HMP1) [40] and the sequence data processed by Deblur [41] in the first release of the Earth Microbiome Project (EMP) [42]. The 16S rRNA GCN for each OTU in the HMP1 and EMP datasets was predicted using *RasperGade16S*. We picked 2560 samples in the HMP1 dataset with complete metadata and used the 2000-sample subset of EMP, and determined the adjusted NSTI and relative cell abundance in each community as described above. For beta-diversity, we randomly picked 100 representative samples from each of the 5 body sites in the HMP1 dataset and analyzed their beta-diversity as described above. For the EMP dataset, we analyzed the beta-

diversity within each level-2 EMP ontology (EMPO) category (around 400 to 600 samples per category).

Examining the adjusted NSTI of empirical bacterial communities

To check the predictability of 16S rRNA GCN in empirical data, we examined bacterial communities surveyed by 16S rRNA amplicon sequencing in the MGnify resource platform [43] that were processed with the latest two pipelines (4.1 and 5.0). The MGnify resource platform uses the SILVA database release 132 [1] for OTU-picking in their latest pipelines, and therefore predicted GCNs for SILVA OTUs can be used directly. We filtered the surveyed communities from the MGnify platform so that only communities with greater than 80% of their gene reads mapped to the SILVA reference at a similarity of 97% or greater were included. This filtering yielded 113842 bacterial communities representing a broad range of environment types. We calculated the adjusted NSTI for each community and examined the adjusted NSTI distribution in various environmental types.

Results

Time-independent variation is present in 16S rRNA GCN evolution

To evaluate the extent of intraspecific variation in 16S rRNA GCN, we examined 5437 pairs of genomes with identical 16S rRNA gene alignments. The 16S rRNA GCN differs in 607 (11%) of them, suggesting the presence of significant intraspecific variation or time-independent variation. Using AIC, we found that incorporating time-independent variation with the BM model greatly improves the model fit (Table 1), indicating the necessity to take time-independent variation into account in 16S rRNA GCN prediction. In addition, we observed that the rate of evolution in the

fitted BM model is inflated by 1670 folds when time-independent variation is not included in the model. Such inflation in the estimated rate of evolution will lead to overestimation of uncertainty in the 16S rRNA GCN prediction.

Table 1. The AICs of Brownian motion model and pulsed evolution model.

Model	BM	BM (with time-independent variation)	PE (with time-independent variation)
Homogenous model	34338	18028	-7925
Heterogeneous model	NA	NA	-15395

Pulsed evolution model explains the 16S rRNA GCN evolution better than the Brownian motion model

When predicting traits using phylogenetic methods, the BM model is commonly assumed to be the model of evolution. We have shown that PE model is a better model for explaining the evolution of [14,20] bacterial genome size [37], prompting us to test whether pulsed evolution can be applied to explain 16S rRNA GCN evolution as well. Using the R package *RasperGade* that implements the maximum likelihood framework of pulsed evolution described by Landis and Schraiber [14], we fitted the PE model with time-independent variation to the same dataset. Table 1 shows that the PE model provides a significantly better fit than the BM model, indicating that 16S rRNA GCN prediction should assume the PE model instead of the BM model. Fitted model parameters are not sensitive to the HMM profiles used for aligning the 16S rRNA sequences (Table S2).

Substantial rate heterogeneity exists in 16S rRNA GCN evolution

To systematically examine the rate heterogeneity of 16S rRNA GCN evolution in the reference genomes, we first used the variance of PICs as an approximate estimate of the local evolution rate of 16S rRNA GCN. We found that the rate of evolution varies greatly among genera (Figure S1), but can be roughly divided into two groups with high and low rates of evolution. Therefore, we developed a heterogeneous pulsed evolution model where all jumps are the same size but the frequency of jumps varies between two groups to accommodate the heterogeneity among different bacterial lineages. Using a likelihood framework and AIC, we classified 3049 and 3358 nodes and their descending branches into slowly-evolving and regularly-evolving groups respectively (Figure S2). The frequency of jumps in the regularly-evolving group is 145 folds of the frequency in the slowly-evolving group (Table S3). The heterogeneous PE model provides the best fit among all models tested (Table 1), indicating that a heterogeneous PE model should be assumed in predicting 16S rRNA GCN.

Apart from the rate of pulsed evolution, we also observed heterogeneity in time-independent variation: for the slowly-evolving group, the fitted model parameters indicate no time-independent variation, while for the regularly-evolving group, the magnitude of time-independent variation is approximately 40% of a jump in pulsed evolution (Table S3). The presence of time-independent variation caps the confidence of prediction in the regularly-evolving group at 85%, which can only be achieved when the query has identical 16S rRNA gene alignment to one of the reference genomes.

The effect of NSTD on accuracy and uncertainty of 16S rRNA GCN predictions

Because of the stochastic nature of evolution, the inherent uncertainty in hidden state prediction accumulates over time, and consequently the accuracy of the prediction decreases as the phylogenetic distance to the reference increases [12]. To get a better understanding of the relationships between NSTD and metrics that measure the accuracy and uncertainty of the prediction, we performed a cross-validation experiment using simulated datasets. We simulated the evolution of 16S rRNA GCN under the fitted heterogeneous pulsed evolution model along the reference phylogeny (ST1), and predicted the simulated GCN of the tips using different methods: the pulsed evolution model (PE), the BM model (pic), maximum parsimony (mp) and empirical probability (emp). As expected, we found that the true uncertainty of the prediction, as predicted by the pulsed evolution model under which the simulated GCN evolves, increases with the NSTD. The true confidence of the prediction, calculated as 1 - uncertainty, decreases with the NSTD (Figure 1A, purple line). The pic method predicts greatly inflated uncertainty (Figure 1A, red line), while the mp method predicts no uncertainty at all (Figure 1A, blue line). The emp method predicts intermediate uncertainty that is greater than the true uncertainty at small NSTDs, but smaller than the truth at large NSTDs (Figure 1A, green line). We used the coefficient of determination (R^2) of the predicted trait values to the truth to evaluate the accuracy of the prediction. Figure 1B shows the PE method performs the best. It is followed by the mp and the pic method. The emp method performs the worst. As observed in previous research [12], the accuracy decreases as the NSTD increases (Figure 1B).

Because we will use the uncertainty measure to evaluate the reliability of the prediction, we tested whether the uncertainty predicted by the various methods we compared here captures the

true reliability of the prediction. Specifically, we calculated the precision and recall of predictions with a confidence of 95% or greater to examine the recovery of highly reliable predictions. We define precision as the proportion of accurately predicted 16S rRNA GCN in predictions with ≥ 95% confidence, and recall as the proportion of predictions with ≥ 95% confidence in the accurately predicted 16S rRNA GCNs. Ideally, the precision should be greater than 95% throughout the NSTD spectrum, while the recall should gradually drop as the NSTD and the uncertainty of prediction increase. We found that the PE method yields high recall at small NSTDs and it decreases as NSTD and uncertainty in the prediction increase (Figure 1C, purple line). In terms of precision, the PE method yields high precision throughout the spectrum of NSTD (Figure 1D, purple line). The pic method has the lowest recall rate at the smallest NSTD and no recovery beyond as it overestimates the uncertainty (Figure 1C and D, red lines). On the contrary, the mp method yields the highest recall regardless of NSTD as it predicts no uncertainty at all (Figure 1C, blue line), but it suffers from lower precision than the PE method and the precision drops quickly as NSTD increases (Figure 1D, blue line). In essence, the uncertainty estimated using the pic method is so great that few predictions can be trusted. On the other hand, according to the mp method, there is no uncertainty in a prediction and every prediction is reliable. The emp method shows a similar trend in recall compared to the PE method, but suffers from lower precision than the PE method.

In summary, the uncertainty of 16S rRNA GCN prediction increases with the increase of NSTD, and as a result, the accuracy of prediction drops as the NSTD increases for all methods. The recall rate of highly reliable predictions also drops with the increasing NSTD and uncertainty, while the precision can remain high throughout the NSTD spectrum.

RasperGade16S improves confidence estimate for 16S rRNA GCN prediction in empirical data

Using 16S rRNA GCN from the 6408 complete genomes in the reference phylogeny for cross-validation, we compared the performance of various methods in accuracy and confidence estimates. In general, the trends of uncertainty, accuracy, precision and recall plotted against the NSTD (Figure 2) are very similar to those observed in the simulation study (Figure 1), indicating that *RasperGade16S* models the 16S rRNA GCN evolution reasonably well. As observed in the simulation, the pic and mp methods produce very large and zero uncertainty respectively (Figure 2A), leading to both poor precision and recall rates (Figure 2C and 2D). The emp method performs the worst in terms of accuracy. The PE method produces the best overall precision, achieving an average precision rate of 0.96 throughout the NSTD spectrum. Overall, the PE method provides one of the best accuracies and the best confidence estimate for 16S rRNA GCN prediction over the full spectrum of NSTD, and should be preferred when predicting 16S rRNA GCN.

As NSTD of the 16S rRNA gene also depends on the sequence alignment and how it is trimmed, it can vary from study to study using the same set of reference sequences. Therefore, to put NSTD values of this study in a taxonomic context, we calculated the NSTDs between taxa at different taxonomical levels. For example, at the species level, we calculated the NSTD of a species to another species within the same genus. We found that the median NSTD between congeneric species is around 0.01 substitutions/site and the maximum NSTD threshold (0.464 substitutions/site) in our cross-validation experiment roughly correspond to a taxonomic distance somewhere between class and order (Figure S3).

Copy number correction improves relative cell abundance estimation

Because 16S rRNA GCN variation biases gene abundances disproportionately among the community members, it distorts the relative cell abundance estimated from the gene abundance [5]. From theoretical calculations, in general, community members with lower relative cell abundances suffer from greater impacts by 16S rRNA GCN variation, while those with higher relative cell abundances appear to be less affected by it (Figure 3A). The impact of 16S rRNA GCN variation also depends on the deviation of a member's GCN from the average GCN of the community members, with larger deviations resulting in larger impacts (Figure 3A). When a member's 16S rRNA GCN is greater than the average GCN of the community, its relative abundance will be overestimated. On the other hand, when a member's 16S rRNA GCN is smaller than the average GCN, its relative abundance will be underestimated. In simulated dataset SC1, we found that 16S rRNA GCN variation has a large detrimental effect on the estimated relative cell abundance (Figure 3B). On average, the relative cell abundance estimated using the gene abundance increased or decreased by 1.8-fold compared to the true relative cell abundance, and the empirical probability of correctly identifying the most abundant OTU based on the gene abundance is only around 13% (Figure 3C). Correcting for 16S rRNA GCN improves the estimated relative cell abundance (Figure 3B). As expected, the improvement is greatest when the adjusted NSTI is small (i.e., when there are closely related reference genomes), and it gradually diminishes when the adjusted NSTI increases. At the smallest adjusted NSTI, the average fold change of the estimated relative cell abundance decreases to 1.1-fold after 16S rRNA GCN correction and the empirical probability of correctly identifying the most abundant OTU increases to around 65% (Figure 3C).

Because we predict each OTU's 16S rRNA GCN with a confidence estimate, we can provide 95% confidence intervals (95% CIs) for their relative cell abundance as well. Ideally, 95% of the true relative cell abundances should be covered by the 95% CIs. Figure 3D shows that the average coverage probability of the true relative cell abundance is about 98% across NSTD cutoffs, indicating that our 95% CIs are slightly over-conservative. Similarly, we can also calculate the coverage probability of our 95% CI to the relative gene abundance. As expected, when the coverage probability to the relative gene abundance increases, the improvement by GCN correction (quantified by the relative reduction in the difference between the estimated and true cell abundances) decreases (Figure 3E), and that when this coverage probability is below 95%, GCN correction always results in strong improvement in relative cell abundance estimates. In empirical studies when the true abundance is unknown, we can use the coverage probability to the relative gene abundance as a conservative statistic to decide if GCN correction for a community will likely improve the relative abundance estimation or not. For the most abundant OTU in the community, we can calculate its support value from the 16S rRNA GCN's confidence estimates. We found that the calculated support value matches the empirical probability that the most abundant OTU is correctly identified (Figure 3C).

To demonstrate the effect of 16S rRNA GCN correction in empirical data, we analyzed the data from the first phase of the Human Microbiome Project (HMP1) and the 2000-sample subset of Earth Microbiome Project (EMP). We found that on average the relative cell abundance with and without 16S rRNA GCN correction changes around 1.3-fold in HMP1 and 1.6-fold in EMP. Using 95% CIs, we found that less than 18% of the HMP1 samples and less than 10% of the

EMP samples have a coverage probability to the relative gene abundance greater than 95% (Figure 3F), suggesting that 16S rRNA GCN correction will likely improve the estimated relative cell abundances in the vast majority of the HMP1 and EMP samples. In terms of the most abundant OTU, we found that the identity of the most abundant OTU changes after copy number correction in around 20% and 31% of the communities in HMP1 and EMP respectively. The support values for the most abundant OTUs are around 0.85 on average in both datasets, indicating high confidence in the identification of the most abundant OTUs.

Copy number correction provides limited improvements on beta-diversity analyses

Because 16S rRNA GCN variation affects the estimated relative cell abundances, it may also affect the beta-diversity analyses such as PCoA, PERMANOVA, and the random forest test that use the relative cell abundance information. To examine the effect of 16S rRNA GCN variation on these analyses, we simulated communities at different turnover rates in two types of environments where from 0.25% to 5% of the OTUs are enriched in one environment compared to the other (the SC2 dataset). We performed beta-diversity analyses on the simulated data and generated the PCoA plots (an example is given in Figure 4). We found that when the relative gene abundance is used to calculate the Bray-Curtis dissimilarity, the positions of the samples in the PCoA plot shift from their positions based on the true relative cell abundance (solid lines in Figure 4). Correcting for 16S rRNA GCN reduces about 60% of the shift in the dissimilarity space ($P<0.001$, paired t-test, Figure 4). Despite the shift in the PCoA plot, we found that the clustering of communities does not seem to be affected by the 16S rRNA GCN variation.

In addition to the PCoA plot, we observed a limited effect of 16S rRNA GCN variation on other beta-diversity analyses. In PERMANOVA, depending on the signature OTU numbers and turnover rates, the proportion of variance explained (PVE) by the environmental type using the true cell abundances ranges from 6.25 to 17.20% on average. Using gene abundance, the average PVE ranges from 6.27 to 17.22% and the change in PVE is not statistically significant ($P>0.010$, paired t-test with Bonferroni correction, $\alpha=1.85\times10^{-3}$, Table S4), indicating that PERMANOVA is not very sensitive to 16S rRNA GCN variation.

It is a common practice to compare the relative cell abundance of OTUs of interest between environments. We found that such comparison is also not sensitive to 16S rRNA GCN variation (Table S4), with the fold-change of relative cell abundance estimated using the gene abundance and the truth highly concordant ($R^2 > 0.99$). For the top OTUs with the highest fold-change in true cell abundance (i.e., signature OTUs), on average more than 98% of them are also the top OTUs with highest fold-change in gene abundance, indicating that abundance difference across environments is not sensitive to 16S rRNA GCN variation. Alternatively, we can use the random forest test to identify OTUs that are differentially abundant between environments by their importance scores (defined as the mean decrease in classification accuracy if removed from the data). We found that the top OTUs ranked by the importance score recovers from 20.0% to 89.0% of the signature OTUs when the true cell abundances were used (Table S4). When the gene abundances were used, this recovery rate changes to from 18.0% to 89.32% (Table S4), and the change is not statistically significant ($P > 0.032$, paired t-test with Bonferroni correction, $\alpha=1.85\times10^{-3}$). Correcting for 16S rRNA GCN changes the recovery rate to from 17.8% to 89.2%

(Table S4), and the change is not significant either ($P>0.041$, paired t-test with Bonferroni correction, $\alpha=1.85\times10^{-3}$).

To examine the effect of 16S rRNA GCN variation correction on beta-diversity in empirical data, we analyzed the beta-diversity using the HMP1 and EMP datasets. We found that correction of 16S rRNA GCN does not seem to affect the clustering of communities by body sites in the HMP1 PCoA plot. Pairwise PERMANOVA shows that the mean PVE by the body site in HMP1 is 14.9% before 16S rRNA GCN correction and decreases marginally to 14.6% after correction, and the PVEs using the gene abundance and the corrected cell abundance are also highly concordant ($R^2>0.98$). In EMP, within each level-2 environment (EMPO2), the average PVE by level-3 environment (EMPO3) remains at 7.7% before and after 16S GCN correction and the PVEs using the gene abundance and the corrected cell abundance are highly concordant ($R^2>0.99$) as well. On the other hand, pairwise random forest tests yield similar results before and after 16S rRNA GCN correction, with around 9 out of the top 10 features identified by the random forest test remaining unchanged before and after correction in HMP1 and around 8 out of the top 10 unchanged in EMP. In terms of the fold-change of relative cell abundances between body sites, we found that copy number correction has little impact as the estimated fold-change before and after correction are highly similar ($R^2>0.95$) in both datasets.

Predicting 16S rRNA GCNs for SILVA OTUs

Using *RasperGade16S*, we predicted the 16S rRNA GCN for 592605 bacterial OTUs (99% identity) in the release 132 of the SILVA database. Overall, the median adjusted NSTD for all bacterial OTUs is 0.070 substitutions/site, and 34.7% of the predictions have a high confidence

of 95% or greater, and 74.9% of the predictions have a moderate confidence of 50% or greater (Table 2). This shows that for most OTUs in the SILVA database, the phylogenetic distance to a reference 16S rRNA is small enough that we can have reasonable confidence in the predictions. In comparison, randomly guessing has a null confidence of around 6.7% (1 out of 15 possible GCNs). Among major phyla with more than 10000 OTUs, the proportion of highly confident predictions varies greatly (Table 2), with Cyanobacteria having the lowest proportion of 19.1% and Acidobacteria having the highest proportion of 50.4%. Similarly, the proportion of moderately confident predictions varies from 58.3% to 89.5% among these phyla. Interestingly, the proportions of highly confident predictions closely match the proportions of slowly-evolving OTUs in each phylum (Table 2), suggesting a causal relationship between them.

Table 2. Summary of SILVA 16S rRNA GCN predictions.

Taxonomic group	Number of OTUs	Median adjusted NSTD (substitutions/site)	Proportion of OTUs in slowly-evolving group	Proportion of highly confident predictions	Proportion of moderately confident predictions
Bacteria	592605	0.070	34.9%	34.7%	74.9%
Proteobacteria	238929	0.062	43.4%	43.1%	85.4%
Firmicutes	149757	0.091	21.6%	21.5%	68.9%
Actinobacteria	60510	0.061	45.2%	45.2%	89.5%
Bacteroidetes	55663	0.117	29.9%	29.8%	58.3%
Acidobacteria	14534	0.006	50.4%	50.4%	82.7%
Cyanobacteria	13970	0.285	19.9%	19.1%	60.5%

Highly confident predictions are defined as predictions with a confidence of 95% or greater.
Moderately confident predictions are defined as predictions with a confidence of 50% or greater.

Vast majorities of bacterial communities should benefit from copy number correction

To examine if analysis of real communities would benefit from 16S rRNA GCN correction, we calculated the adjusted NSTI for 113842 communities in the microbiome resource platform MGnify (formerly known as EBI Metagenomics) [43] that passed our quality control. These microbiomes were sampled from various environments and include host-associated microbiomes in animals and plants and free-living microbiomes in soil and aquatic environments (Table S5). The adjusted NSTI varies greatly among samples and the median across all samples is 0.01 substitutions/site. For example, the smallest adjusted NSTI (8.2×10^{-7} substitutions/site) comes from a human vaginal clinical sample that is dominated by one OTU (relative cell abundance >0.98). This OTU is closely related to *Lactobacillus iners* in the slowly-evolving group, which results in the extremely small adjusted NSTI. On the other hand, the largest adjusted NSTI (0.6 substitutions/site) belongs to a sample from the rumen of dairy cows. The majority of OTUs in this sample has an adjusted NSTD greater than 0.1 substitutions/site and account for more than 90% of the total cell abundance. In the simulated communities, we observed that GCN correction significantly improves the estimated relative cell abundances ($P<0.001$, paired t-test) even when the adjusted NSTI reaches 0.3 substitutions/site. We found that the vast majority of the communities (>99%) from MGnify have an adjusted NSTI less than 0.3 substitutions/site, suggesting that they should benefit from 16S rRNA GCN correction when estimating the relative cell abundances. The distribution of adjusted NSTI varies among different environmental types (Figure 5), but the proportion of communities that will likely benefit from 16S rRNA GCN correction remains high, ranging from 98% to 100%.

Discussion

16S rRNA GCN variation skews bacterial community composition estimated from the 16S rRNA read count. To correct for the bias introduced by the GCN variation, several methods have been developed to predict GCN from reference genomes. A recent study has pointed out that the GCN predictions come with inherent uncertainty, particularly for these taxa without closely related genomes [12]. The concern is that inaccurate predictions can introduce noise to community compositions that can be worse than the original GCN-related biases, thereby raising doubt about the usefulness of the 16S rRNA GCN correction in bacterial diversity analyses [8,12].

We address the inherent uncertainty problem in 16S rRNA GCN prediction by directly measuring it with confidence estimates. Using simulations and cross-validation, we show that the PE method implemented in *RasperGade16S* outperforms other methods in both the precision and recall rates. This method's strength comes from three features of its modeling of the 16S rRNA GCN evolution: implementation of a pulsed evolution model and accounting for the rate heterogeneity and time-independent trait variation. Pulsed evolution model expects no trait changes to occur over a short branch as jumps are not likely to happen on that branch. This leads to a higher confidence to 16S rRNA GCN prediction with a short NSTD, and thus improves the recall of the accurate predictions. By incorporating rate heterogeneity, we can make predictions in the slowly-evolving groups with high confidence, even when their NSTDs are large, thereby further improving the overall precision and recall rates. In the reference phylogeny, 48% of branches were estimated to fall within this slowly-evolving group, whose evolution rate is 145 times slower compared to that of the regularly-evolving group. The third source of improvement

for *RasperGade16S* comes from accounting for time-independent variation, which can result from measurement error and intraspecific variation. We show that failing to account for time-independent variation results in model misspecification (Table 1) and overestimated rate of evolution for the pic method.

Having confidence estimates is critical in the presence of inherent uncertainty because they provide direct evaluation of the uncertainty associated with the predictions. Although such uncertainty is positively correlated with the NSTD (Figure 2), use of NSTD as a measure of uncertainty lacks a clear statistical meaning. Using cross-validation, we show that *RasperGade16S* has high precision (around 0.96), which means for predictions with high confidence (≥95%), 96% of the predictions are accurate. Therefore, we can use the confidence score provided by *RasperGade16S* to select high-quality predictions if necessary, or we can draw firm conclusions from the 16S rRNA data when the confidence is high. For example, 16S rRNA GCN has been linked to the ecological strategy of bacterial species, with oligotrophs generally having low GCNs and copiotrophs having higher GCNs [17,18]. To better understand the overall ecological strategy of a bacterial community, we can predict its members' GCNs and classify the community into either an oligotroph-dominant, copiotroph-dominant or a mixed community, and we can do this with a measure of confidence.

The application of confidence estimation extends beyond the prediction of 16S rRNA GCN. Because the uncertainty in the prediction is inherited by statistics derived from the predicted 16S rRNA GCN, we can estimate the uncertainty and confidence intervals of important parameters in downstream analyses, such as the relative cell abundance. With confidence intervals, we can

draw more meaningful and sound conclusions, such as identifying the most abundant OTU in the community with a support value. Getting confidence estimates of the relative cell abundance is also important for predicting the functional profile of a community based on 16S rRNA sequences. Although PICRUST2 uses an extremely lenient NSTD cut-off to eliminate problematic sequences, it does not provide an accurate confidence measurement of its predictions. As shown in this study, the default maximum parsimony method used by PICRUST2 to predict 16S rRNA GCN essentially assumes there is no uncertainty in the predictions, which is unrealistic and leads to poor precision. Incorporation of a more meaningful confidence estimate of 16S rRNA GCN prediction in PICRUST2 should make its functional profile prediction more informative.

We predicted GCN for 592605 bacterial OTU99 in the SILVA database. Not surprisingly, we observed considerable uncertainty in the GCN predictions. This is because only a small fraction of bacterial diversity in the SILVA database has been captured by the fully sequenced genomes. In addition, 65.1% of OTUs in SILVA database belong to the regularly-evolving group and the confidence of predictions for these OTUs is capped at 85% because of the time-independent variation. However, we would like to point out that natural communities are not a random subsampling of the SILVA OTUs and the median NSTI (NSTD weighted by community members' relative abundance) of the 113842 bacterial communities we examined is 0.01 substitutions/site, much lower than the median NSTD of SILVA OTUs. Strikingly, 99% of 113842 bacterial communities we examined have an adjusted NSTI less than 0.3 substitutions/site, a range where we show that GCN correction improves the accuracy of the relative cell abundance estimation (Figure 3B). Because these communities represent a

comprehensive and diverse list of natural and engineered environments, we recommend applying 16S rRNA GCN correction to practically any microbial community regardless of the environmental type if accurate estimates of relative cell abundance are critical to the study. Our results therefore affirm the conclusion of the previous studies based on analyses of a much smaller number of communities [5,7].

McLaren et al. have shown that statistics that are functions of individual taxon's relative abundance will be sensitive to the systematic biases introduced in the sequencing and data analysis pipeline (including bias introduced by 16S rRNA GCN variation) [44]. Contrary to some popular belief, these biases will not cancel out when analyzing the differences between samples that have been measured by the same protocol [44]. Nevertheless, few studies have investigated to what extent the bias introduced by 16S rRNA GCN variation will have on the microbiome beta diversity analyses. We show that the effect sizes of 16S rRNA bias on beta-diversity analyses are small. Correcting 16S rRNA GCN provides limited improvement on the beta-diversity analyses such as random forest analysis and PERMANOVA test. One possible reason is that for an OTU, the fold change in the relative cell abundance between samples remains more or less the same with or without correcting for the copy number. For example, assuming the estimated relative cell abundances of an OTU in samples A and B are r_a and r_b respectively without copy number correction. When correcting for the copy number, its relative abundance is adjusted with the scaling factor ACN/GCN, where the GCN is the 16S rRNA copy number of the OTU and the ACN is the average copy number of the sample. Assuming the ACN does not vary much between samples, then the scaling factor for the OTU will be roughly the

same in samples A and B. So even with copy number correction, the relative abundance change will still be close to r_a/r_b.

It should be noted that having a confidence associated with the 16S rRNA GCN prediction helps to estimate the uncertainty of the prediction, but it does not improve the accuracy of the prediction. Accuracy of the prediction is constrained by the inherent uncertainty, which can only be improved by better sampling the reference genomes. However, as our current sampling is inadequate for accurate 16S rRNA GCN prediction of all environmental bacteria, we believe that incorporating confidence estimates is the best practice to control for the uncertainty in the 16S rRNA based bacterial diversity studies, as opposed to not correcting the GCN bias as previously suggested [8,12]. Based on bootstrapping, we have demonstrated that confidence intervals or support values can be calculated for key statistics in downstream analyses such as relative cell abundance and beta diversity. With the uncertainty incorporated into the statistical tests, users may decide if correcting for GCN variation is worthwhile on a case-by-case basis.

Conclusion

We have developed a robust model to estimate the confidence of 16S rRNA GCN predictions. As a rule of thumb, we recommend that, regardless of the environmental type, 16S rRNA GCN correction be applied to virtually all 16S rRNA bacterial communities when estimating their compositional and functional profiles. However, the GCN correction is not necessary for bacterial beta-diversity analyses.

List of abbreviations

16S rRNA: 16S ribosomal RNA. GCN: gene copy number. 16S GCN: 16S rRNA gene copy number. OTU: operational taxonomic unit. BM: Brownian motion. PE: pulsed evolution. PIC: phylogenetically independent contrast. AIC: Akaike information criterion. NSTI: nearest-sequenced-taxon-index. NSTD: nearest-sequenced-taxon-distance. CI: confidence interval. PCoA: principal coordinates analysis. PERMANOVA: permutational multivariate analysis of variance

Declarations

Ethics approval and consent to participate

Not applicable.

Consent for publication

Not applicable.

Availability of data and material

The NCBI accession numbers of the reference genomes, the representative 16S rRNA sequences and alignments, the reference phylogeny, the predicted GCN for OTU99 in the SILVA database, and the simulated bacterial community data generated during the current study are available in the Dryad repository (https://datadryad.org/stash/share/OaS9BjM_kIVdJ3WkZRT7KO8fDr8D4k8jy3LsOtlYELM). The R package *RasperGade16S* can be downloaded from https://github.com/wu-lab-uva/RasperGade16S. The original scripts to conduct the analyses in this study are available in the GitHub repository (https://github.com/wu-lab-uva/16S-rRNA-GCN-Predcition).

Competing interests

The authors declare that they have no competing interests.

Funding

Not applicable

Authors' contributions

YG developed the R package *RasperGade16S*, conducted statistical analyses in the manuscript and was a major contributor in writing the manuscript. MW conceptualized the rate heterogeneity model and was a major contributor in writing the manuscript. Both authors read and approved the final manuscript.

Acknowledgement

Not applicable.

References

1. Quast C, Pruesse E, Yilmaz P, Gerken J, Schweer T, Yarza P, et al. The SILVA ribosomal RNA gene database project: improved data processing and web-based tools. Nucleic Acids Research. 2012;41:D590–6.
2. DeSantis TZ, Hugenholtz P, Larsen N, Rojas M, Brodie EL, Keller K, et al. Greengenes, a chimera-checked 16S rRNA gene database and workbench compatible with ARB. Applied and Environmental Microbiology. 2006;72:5069–72.
3. Klappenbach JA. rrndb: the ribosomal RNA operon copy number database. Nucleic Acids Research. 2001;29:181–4.
4. Větrovský T, Baldrian P. The variability of the 16S rRNA gene in bacterial genomes and its consequences for bacterial community analyses. PLoS ONE. 2013;8:e57923.

5. Kembel SW, Wu M, Eisen JA, Green JL. Incorporating 16S gene copy number information improves estimates of microbial diversity and abundance. PLoS Computational Biology. 2012;8:16–8.
6. McLaren MR, Willis AD, Callahan BJ. Consistent and correctable bias in metagenomic sequencing experiments. Elife. 2019;8.
7. Angly FE, Dennis PG, Skarshewski A, Vanwonterghem I, Hugenholtz P, Tyson GW. CopyRighter: a rapid tool for improving the accuracy of microbial community profiles through lineage-specific gene copy number correction. Microbiome. 2014;2:11.
8. Starke R, Pylro VS, Morais DK. 16S rRNA gene copy number normalization does not provide more reliable conclusions in metataxonomic surveys. Microbial Ecology. 2021;81.
9. Bowman JS, Ducklow HW. Microbial communities can be described by metabolic structure: A general framework and application to a seasonally variable, depth-stratified microbial community from the coastal west Antarctic peninsula. PLOS ONE. 2015;10:e0135868.
10. Langille MGI, Zaneveld J, Caporaso JG, McDonald D, Knights D, Reyes JA, et al. Predictive functional profiling of microbial communities using 16S rRNA marker gene sequences. Nature Biotechnology. 2013;31:814–21.
11. Zaneveld JRR, Thurber RL V. Hidden state prediction: a modification of classic ancestral state reconstruction algorithms helps unravel complex symbioses. Frontiers in Microbiology. 2014;5:431.
12. Louca S, Doebeli M, Parfrey LW. Correcting for 16S rRNA gene copy numbers in microbiome surveys remains an unsolved problem. Microbiome. 2018;6:41.
13. Ané C. Analysis of comparative data with hierarchical autocorrelation. The Annals of Applied Statistics. 2008;2:1078–102.
14. Landis MJ, Schraiber JG. Pulsed evolution shaped modern vertebrate body sizes. Proceedings of the National Academy of Sciences. 2017;114:13224–9.
15. Joy JB, Liang RH, McCloskey RM, Nguyen T, Poon AFY. Ancestral reconstruction. PLOS Computational Biology. 2016;12:e1004763.
16. Elliot MG, Mooers AØ. Inferring ancestral states without assuming neutrality or gradualism using a stable model of continuous character evolution. BMC Evolutionary Biology. 2014;14:226.
17. Roller BRK, Stoddard SF, Schmidt TM. Exploiting rRNA operon copy number to investigate bacterial reproductive strategies. Nature Microbiology. 2016;1:1–7.
18. Lauro FM, McDougald D, Thomas T, Williams TJ, Egan S, Rice S, et al. The genomic basis of trophic strategy in marine bacteria. Proceedings of the National Academy of Sciences. 2009;106:15527–33.
19. Eldredge N, Gould SJ. Punctuated equilibria - an alternative to phyletic gradualism. Models in Paleobiology. 1972. p. 82–115.
20. Uyeda JC, Hansen TF, Mcpeek A. The million-year wait for macroevolutionary bursts. Proceedings of the National Academy of Sciences. 2011;108:15908–13.

21. Yano K, Masuda K, Akanuma G, Wada T, Matsumoto T, Shiwa Y, et al. Growth and sporulation defects in Bacillus subtilis mutants with a single rrn operon can be suppressed by amplification of the rrn operon. Microbiology. 2016;162:35–45.
22. Rastogi R, Wu M, DasGupta I, Fox GE. Visualization of ribosomal RNA operon copy number distribution. BMC Microbiology. 2009;9:208.
23. Stoddard SF, Smith BJ, Hein R, Roller BRK, Schmidt TM. rrnDB: Improved tools for interpreting rRNA gene abundance in bacteria and archaea and a new foundation for future development. Nucleic Acids Research. 2015;43.
24. Sadeghifard N, Gu□rtler V, Beer M, Seviour RJ. The mosaic nature of intergenic 16S-23S rRNA spacer regions suggests rRNA operon copy number variation in Clostridium difficile strains. Applied and Environmental Microbiology. 2006;72:7311–23.
25. Lee CM, Sieo CC, Abdullah N, Ho YW. Estimation of 16S rRNA gene copy number in several probiotic Lactobacillus strains isolated from the gastrointestinal tract of chicken. FEMS Microbiology Letters. 2008;287:136–41.
26. Bodilis J, Nsigue-Meilo S, Besaury L, Quillet L. Variable copy number, intra-genomic heterogeneities and lateral transfers of the 16S rRNA gene in Pseudomonas. PLoS ONE. 2012;7:e35647.
27. Lavrinienko A, Jernfors T, Koskimäki JJ, Pirttilä AM, Watts PC. Does intraspecific variation in rDNA copy number affect analysis of microbial communities? Trends in Microbiology. 2021;29:19–27.
28. Viklund J, Ettema TJG, Andersson SGE. Independent genome reduction and phylogenetic reclassification of the oceanic SAR11 clade. Molecular Biology and Evolution. 2012;29.
29. Moran NA. Accelerated evolution and Muller's rachet in endosymbiotic bacteria. Proceedings of the National Academy of Sciences. 1996;93:2873–8.
30. Wu D, Hugenholtz P, Mavromatis K, Pukall R, Dalin E, Ivanova NN, et al. A phylogeny-driven genomic encyclopaedia of Bacteria and Archaea. Nature. 2009;462.
31. Katoh K, Standley DM. MAFFT multiple sequence alignment software version 7: Improvements in performance and usability. Molecular Biology and Evolution. 2013;30.
32. Perisin M, Vetter M, Gilbert JA, Bergelson J. 16Stimator: statistical estimation of ribosomal gene copy numbers from draft genome assemblies. The ISME Journal. 2016;10:1020–4.
33. Eddy SR. Accelerated profile HMM searches. PLoS Computational Biology. 2011;7:e1002195.
34. Stamatakis A. RAxML version 8: a tool for phylogenetic analysis and post-analysis of large phylogenies. Bioinformatics. 2014;30:1312–3.
35. Torsten Seemann. Barrnap [Internet]. 2018 [cited 2022 Mar 12]. Available from: https://github.com/tseemann/barrnap
36. Felsenstein J. Phylogenies and the comparative method. American Naturalist. 1985;125:1–15.
37. Gao Y, Wu M. Modeling pulsed evolution and time-independent variation improves the confidence level of ancestral and hidden state predictions. Systematic Biology. 2022;

38. Louca S, Doebeli M. Efficient comparative phylogenetics on large trees. Bioinformatics. 2018;34:1053–5.
39. Barbera P, Kozlov AM, Czech L, Morel B, Darriba D, Flouri T, et al. EPA-ng: Massively parallel evolutionary placement of genetic sequences. Systematic Biology. 2019;68:365–9.
40. The Human Microbiome Project Consortium. A framework for human microbiome research. Nature. 2012;486:215–21.
41. Amir A, McDonald D, Navas-Molina JA, Kopylova E, Morton JT, Zech Xu Z, et al. Deblur rapidly resolves single-nucleotide community sequence patterns. mSystems. 2017;2.
42. Thompson LR, Sanders JG, McDonald D, Amir A, Ladau J, Locey KJ, et al. A communal catalogue reveals Earth's multiscale microbial diversity. Nature. 2017;551:457–63.
43. Mitchell AL, Almeida A, Beracochea M, Boland M, Burgin J, Cochrane G, et al. MGnify: the microbiome analysis resource in 2020. Nucleic Acids Research. 2019;48:D570–8.
44. McLaren MR, Willis AD, Callahan BJ. Consistent and correctable bias in metagenomic sequencing experiments. Elife. 2019;8.

Figure legends

Figure 1. The performance of prediction on simulated 16S rRNA GCN. Using cross-validation of simulated data, the mean estimated uncertainty and confidence of predictions (A), the mean coefficient of determination R^2 of the predictions (B), and the recall (C) and precision (D) of classification of predictions by their associated confidence estimate, plotted against the mean NSTD. The red line is missing in D because no predictions under the BM model have ≥ 95% confidence when the mean NSTD is greater than 0.002 substitutions/site. The error bars represent the 95% CI of the mean.

Figure 2. The performance of prediction on empirical 16S rRNA GCN. Using cross-validation of empirical data, the mean estimated uncertainty and confidence of predictions (A), the mean coefficient of determination R^2 of the predictions (B), and the recall (C) and precision (D) of classification of predictions by their associated confidence estimate, plotted against the mean NSTD. The error bars represent the 95% CI of the mean. The empirical 16S rRNA GCN analyzed here are from the 6408 complete genomes in the reference phylogeny.

Figure 3. The impact of 16S rRNA GCN variation on estimated relative cell abundances. (A) The impact of GCN variation on estimated relative cell abundance based on theoretical calculations. The color of the lines denotes the ratio of an OTU's of GCN to the average GCN of the community. (B) The average fold-change to the true relative cell abundance. (C) The empirical probability of correctly identifying the most abundant OTU in the community and the support value for the most abundant OTU. (D) The coverage probability of relative cell abundances' estimated 95% CIs to the true relative cell abundance. (E) The correlation between the coverage probability to the relative gene abundance and the improvement by GCN correction. The horizontal red dashed line represents no improvement in relative cell abundance estimates; the vertical red dashed line represents 95% coverage probability to the relative gene abundance. The improvement is quantified by the relative reduction in the difference between the estimated and true cell abundances. (F) The empirical cumulative distribution of the coverage probability to the relative gene abundance in 2560 samples from the HMP1 dataset and 1856 samples from the EMP dataset. All error bars represent 95% CI of the mean.

Figure 4. The impact of 16S rRNA GCN variation on beta-diversity. Example of shift in the Bray-Curtis dissimilarity matrix due to 16S rRNA GCN variation. The shift is visualized in a PCoA plot comparing 20 simulated samples from two hypothetical environments with 5 signature OTUs in each environment and a turnover rate of 30%. Solid lines represent the shift of a sample from its true location when using the gene abundance.

Figure 5. The distribution of adjusted NSTI in empirical data. The distribution of adjusted NSTI of 113842 communities in the MGnify database representing various environmental types. The red dashed line marks the adjusted NSTI of 0.3 substitutions/site.

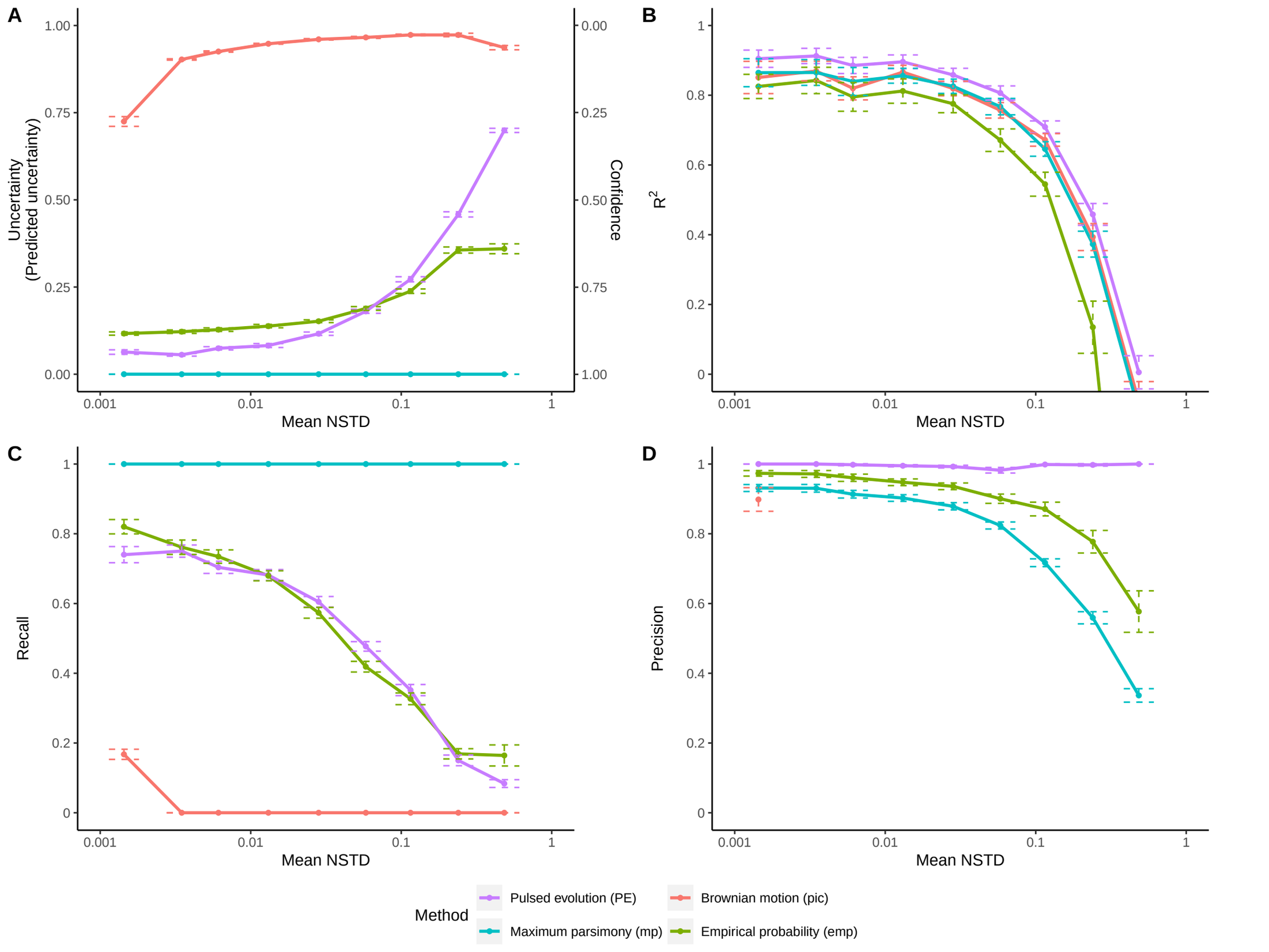
A
Uncertainty
(Predicted uncertainty)
Confidence
Mean NSTD
B
R^2
Mean NSTD
C
Recall
Mean NSTD
D
Precision
Mean NSTD
Method
Pulsed evolution (PE)
Brownian motion (pic)
Maximum parsimony (mp)
Empirical probability (emp)

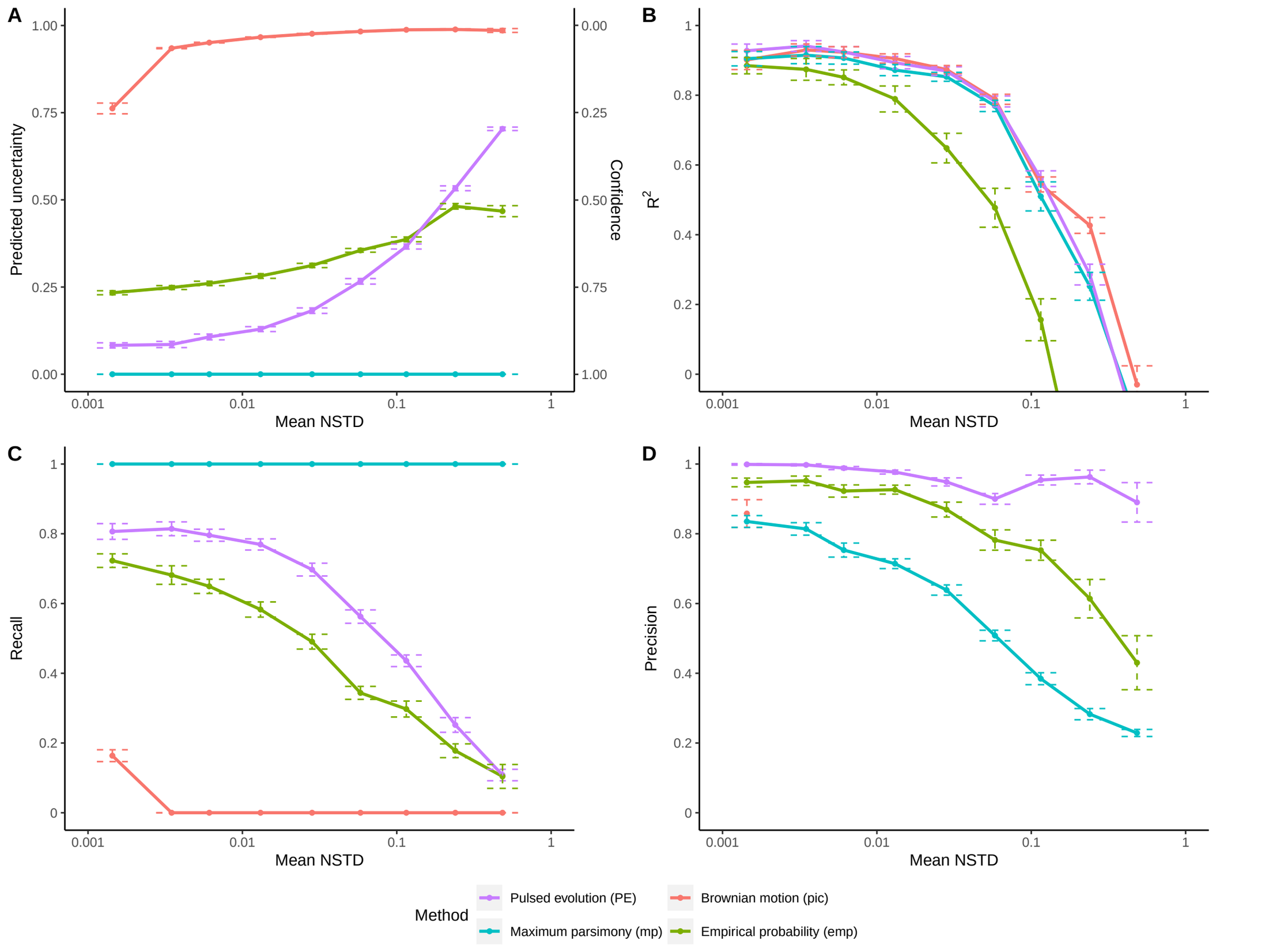
A
Predicted uncertainty
Confidence
Mean NSTD
B
R^2
Mean NSTD
C
Recall
Mean NSTD
D
Precision
Mean NSTD
Method
Pulsed evolution (PE)
Brownian motion (pic)
Maximum parsimony (mp)
Empirical probability (emp)

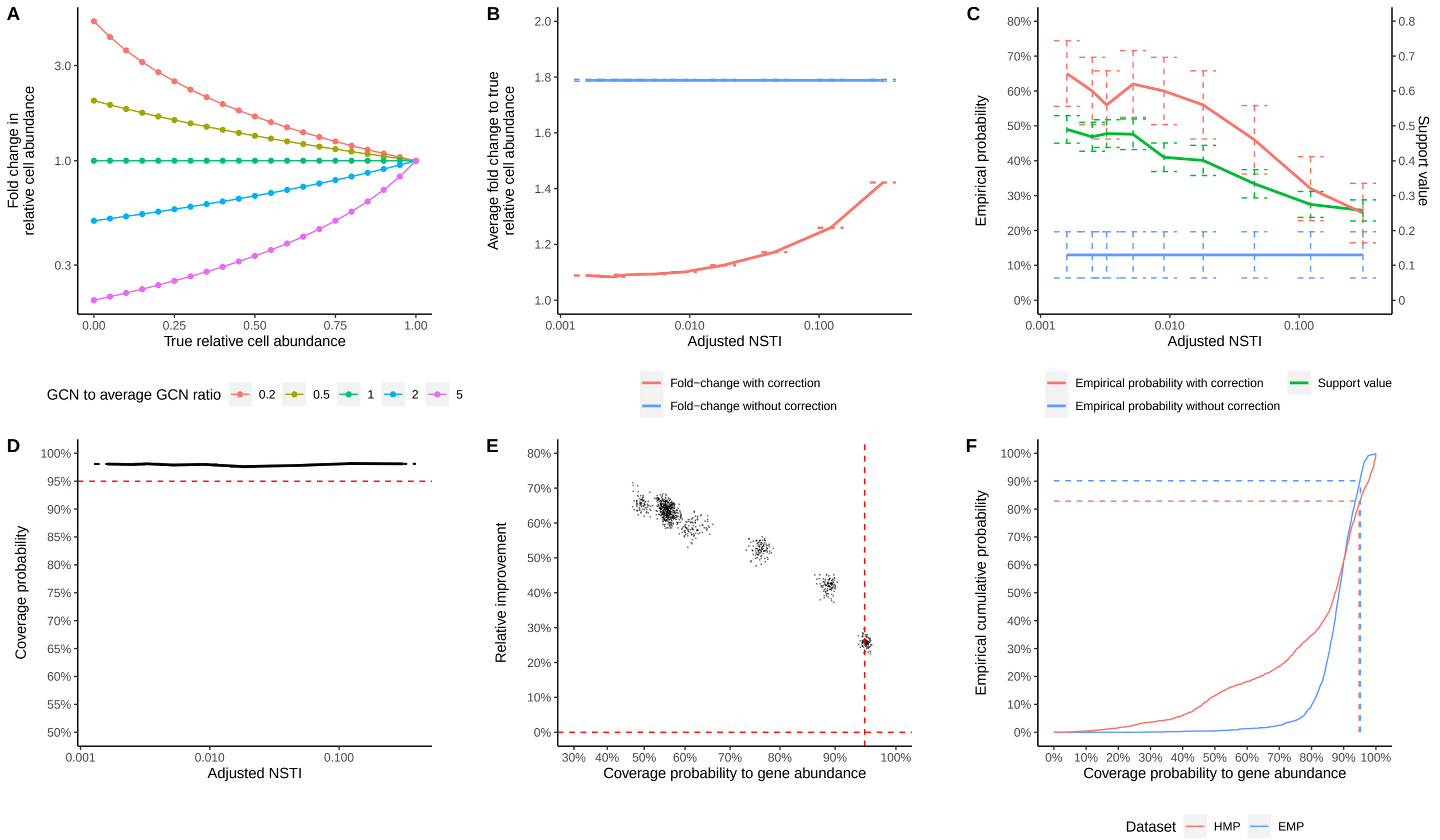
A
Fold change in relative cell abundance
3.0
1.0
0.3
0.00
0.25
0.50
0.75
1.00
True relative cell abundance
GCN to average GCN ratio
0.2
0.5
1
2
5
B
Average fold change to true relative cell abundance
2.0
1.8
1.6
1.4
1.2
1.0
0.001
0.010
0.100
Adjusted NSTI
Fold−change with correction
Fold−change without correction
C
Empirical probability
80%
70%
60%
50%
40%
30%
20%
10%
0%
Support value
0.8
0.7
0.6
0.5
0.4
0.3
0.2
0.1
0
0.001
0.010
0.100
Adjusted NSTI
Empirical probability with correction
Empirical probability without correction
Support value
D
Coverage probability
100%
95%
90%
85%
80%
75%
70%
65%
60%
55%
50%
0.001
0.010
0.100
Adjusted NSTI
E
Relative improvement
80%
70%
60%
50%
40%
30%
20%
10%
0%
30%
40%
50%
60%
70%
80%
90%
100%
Coverage probability to gene abundance
F
Empirical cumulative probability
100%
90%
80%
70%
60%
50%
40%
30%
20%
10%
0%
0%
10%
20%
30%
40%
50%
60%
70%
80%
90%
100%
Coverage probability to gene abundance
Dataset
HMP
EMP

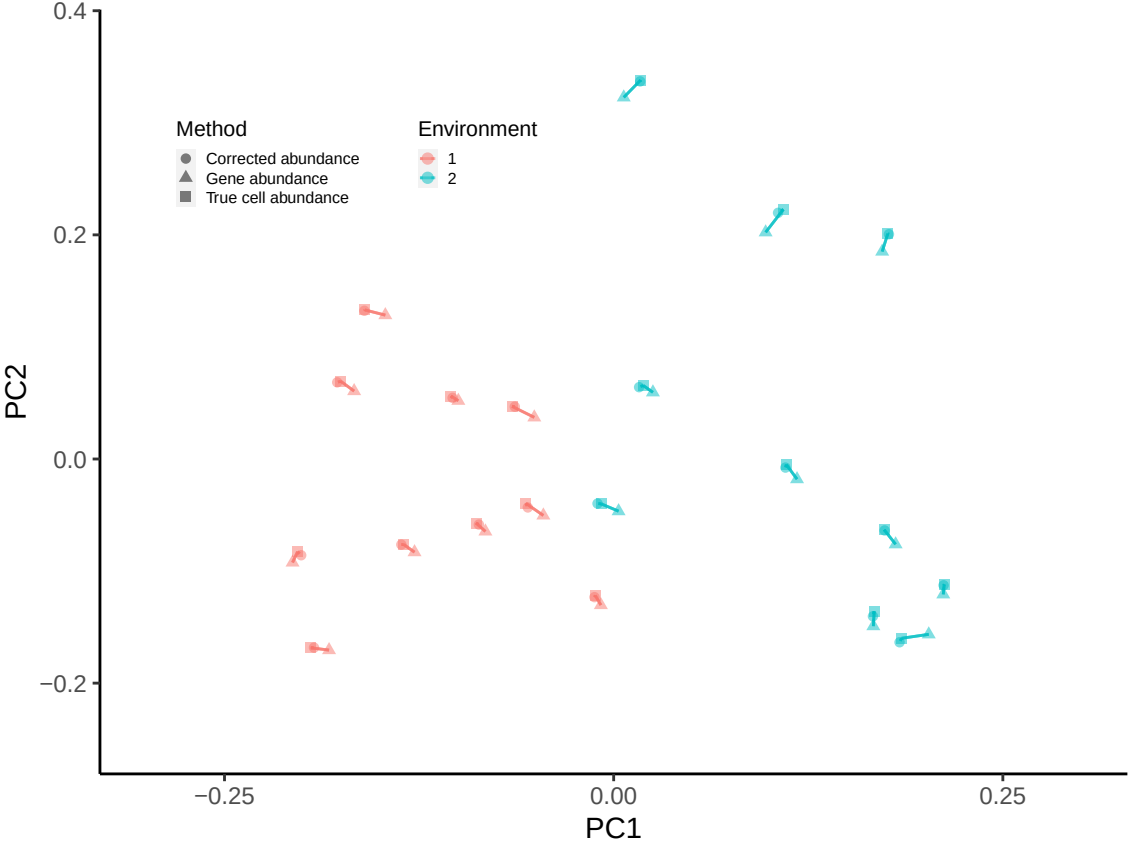
Method
Corrected abundance
Gene abundance
True cell abundance
Environment
1
2
0.4
0.2
0.0
−0.2
PC2
−0.25
0.00
0.25
PC1

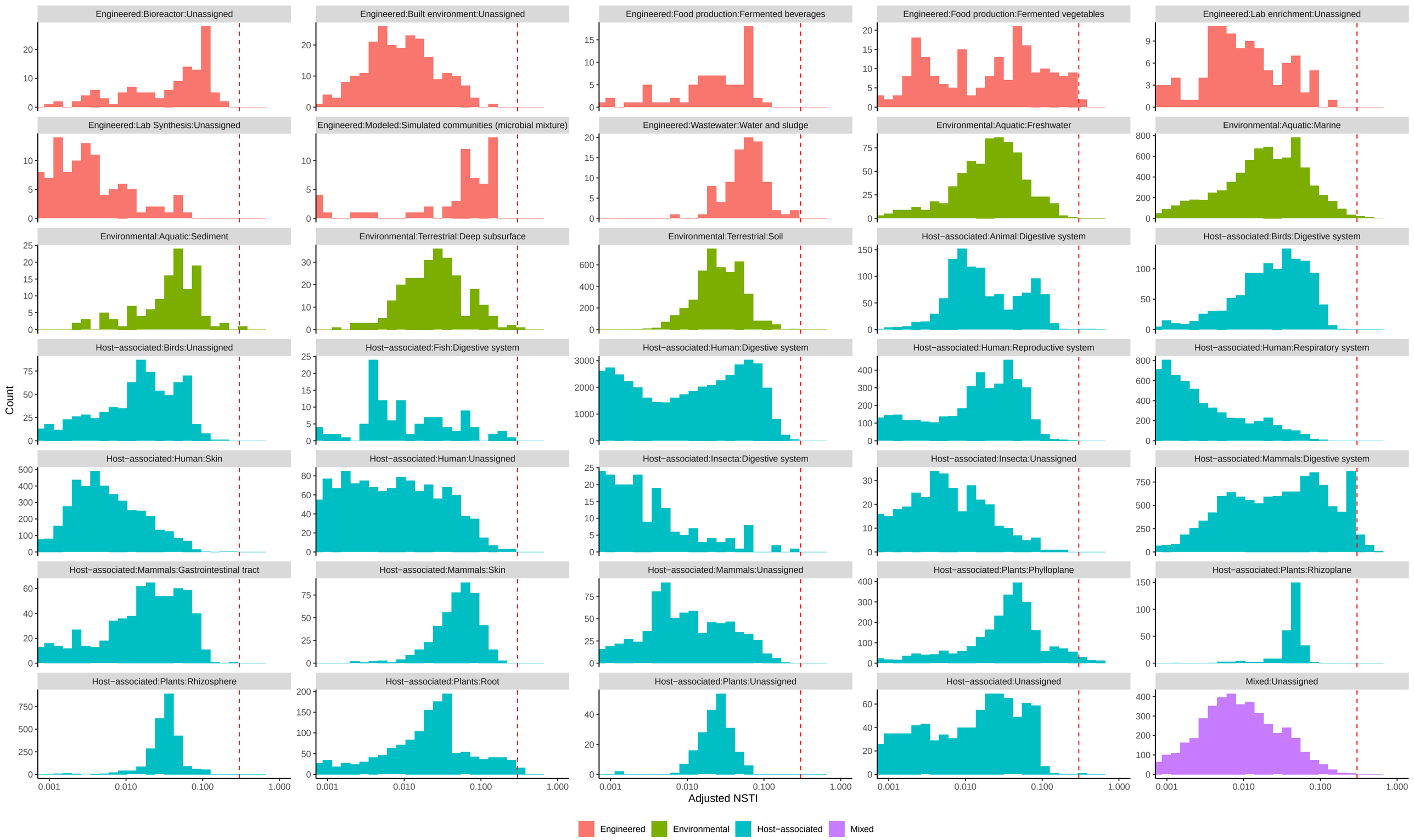
Engineered:Bioreactor:Unassigned
Engineered:Built environment:Unassigned
Engineered:Food production:Fermented beverages
Engineered:Food production:Fermented vegetables
Engineered:Lab enrichment:Unassigned
Engineered:Lab Synthesis:Unassigned
Engineered:Modeled:Simulated communities (microbial mixture)
Engineered:Wastewater:Water and sludge
Environmental:Aquatic:Freshwater
Environmental:Aquatic:Marine
Environmental:Aquatic:Sediment
Environmental:Terrestrial:Deep subsurface
Environmental:Terrestrial:Soil
Host−associated:Animal:Digestive system
Host−associated:Birds:Digestive system
Host−associated:Birds:Unassigned
Host−associated:Fish:Digestive system
Host−associated:Human:Digestive system
Host−associated:Human:Reproductive system
Host−associated:Human:Respiratory system
Host−associated:Human:Skin
Host−associated:Human:Unassigned
Host−associated:Insecta:Digestive system
Host−associated:Insecta:Unassigned
Host−associated:Mammals:Digestive system
Host−associated:Mammals:Gastrointestinal tract
Host−associated:Mammals:Skin
Host−associated:Mammals:Unassigned
Host−associated:Plants:Phylloplane
Host−associated:Plants:Rhizoplane
Host−associated:Plants:Rhizosphere
Host−associated:Plants:Root
Host−associated:Plants:Unassigned
Host−associated:Unassigned
Mixed:Unassigned
Count
Adjusted NSTI
0.001
0.010
0.100
1.000
Engineered
Environmental
Host−associated
Mixed